CHIN. PHYS. LETT. Vol. 27, No. 8 (2010) 089701

Multiband Non-Thermal Radiation from the Crab Nebula and the Pulsar Wind Nebula in MSH 15–52 *

YU Huan(于欢)[1], JIANG Ze-Jun(姜泽军)[1,2]**

[1]Department of Physics, Yunnan University, Kunming 650091
[2]National Astronomical Observatories/Yunnan Observatory, Chinese Academy of Sciences, Kunming 650011

(Received 16 April 2010)

We study the multiband non-thermal emission from two pulsar wind nebulae (PWNe), the Crab nebula and the PWN in MSH 15–52. Both of them have been recently detected by the Fermi large area telescope (LAT) and powered by central gamma-ray pulsars. Motivated by the Fermi LAT results, we use a simplified time-dependent injection model to study the non-thermal emission from radio to very high energy gamma-ray radiation from these two sources. In this model, the relativistic electrons are accelerated in pulsar magnetosphere and at pulsar wind termination shocks and can be described by a broken power law. Those high energy particles evolve with time and produce non-thermal emission through synchrotron radiation and inverse Compton scattering of soft photons. For Crab nebula, using the GeV emission from 100 MeV to 10 GeV given by Fermi LAT, we can constrain the maximum energy of the electrons and other parameters. The non-thermal emission can be well explained by this model. We also use this model to explain the non-thermal emission from the PWN in MSH 15–52.

PACS: 97. 60. Gb, 97. 60. Bw, 95.,30. Jx DOI: 10.1088/0256-307X/27/8/089701

It is believed that a young pulsar is a powerful accelerator which can accelerate particles to relativistic energies and lose its rotational energy via relativistic winds. The outflows will interact with the surrounding media of the supernova remnant (SNR) and result in a pulsar wind nebula (PWN) and a termination shock. Particles can be accelerated to relativistic energies by the termination shock and produce high energy gamma-ray emission via synchrotron and inverse Compton process, which can produce the observed nonthermal emission from radio to very high-energy γ-rays.[1−5] Most of the Galactic TeV sources are PWNe or SNRs, such as the Crab nebula and the PWN in MSH 15–52.

Both of the Crab nebula and the PWN in MSH 15–52 have a filled-center radio structure[6] and are powered by central gamma-ray pulsars, the Crab pulsar and PSR B1509-58, respectively. The Crab nebula has been detailedly observed in radio, optical, x-ray and γ-ray bands.[7−9] The x-rays[10−12] and very high energy gamma-rays[13,14] from MSH 15–52 have also been detected. The multibands nonthermal radiations can be explained in the framework of the leptonic model, i.e., the relativistic electrons produce the emission from radio to MeV gamma-rays via synchrotron radiation and high energy gamma-rays via inverse Compton scattering off the ambient soft photons.[15]

In the previous observations, the information in GeV bands is limited because there is only one satellite (i.e., EGRET), which can obtain gamma-rays with energies from 100 MeV to tens of GeV. Recently, the observations by the large area telescope (LAT) on Fermi has improved such situation. Both the Crab nebula and the PWN in MSH 15–52 have been detected by Fermi LAT.[16,17] The detected spectrum of the Crab nebula from 100 MeV to 300 GeV can be fitted by two power-law spectra with photon indexes of ~ 3.99 and ~ 1.64, respectively.[16] The first component of the spectrum can be identified as the falling edge of the synchrotron radiation, and the second as the rising edge of the IC emission. For the PWN in MSH 15–52, the spectrum from 1 to 100 GeV is well described as a power law with a spectral index of 1.57 ± 0.30 and a flux above 1 GeV of $\sim 2.91 \times 10^{-9}\,\mathrm{cm^{-1}s^{-1}}$.[17] These results, combined with other multibands observations, can provide better constrains on the emission models.

Motivated by these new observations, we use a time-dependent injection model of PWN developed by Zhang *et al.*[15] to account for the multi-wavelength observation of the Crab nebula and the PWN in MSH 15–52. In this model, the relativistic electrons in the PWN consist of two components, one coming directly from the pulsar magnetosphere and the other from shock acceleration in the PWN. The relativistic electrons evolve with time and produce the multibands non-thermal emissions via synchrotron radiation and inverse Compton process. We first give a brief review about the model of Zhang *et al.*[15] The spectrum of the relativistic electrons injected in a PWN can be assumed as a broken power-law with indices α_1 and α_2 with a break energy E_b,

$$Q(E_e,t) = \begin{cases} Q_0(t)(E_e/E_b)^{-\alpha_1}, & E_e < E_b. \\ Q_0(t)(E_e/E_b)^{-\alpha_2}, & \\ E_b \le E_e \le E_{\max}(t). & \end{cases} \quad (1)$$

Assuming that a fraction of the spin-down power $L(t)$ is transformed into the particles injected in the PWN luminosity, we have $\int Q(E_e,t)E_e dE_e = \eta L(t)$, where

*Supported by the National Natural Science Foundation of China under Grant Nos 10778702 and 10803005, the National Basic Research Program of China under Grant No 2009CB824800, and Yunnan Province under Grant No 2009OC.
**Email: zejunjiang@hotmail.com
© 2010 Chinese Physical Society and IOP Publishing Ltd

η is the conversion efficiency, and $L(t)$ [15] is given as

$$L(t) = L_0\left[1 + \frac{(n-1)P_0^2 L_0 t}{4\pi^2 I}\right]^{-\frac{n+1}{n-1}}, \quad (2)$$

where L_0 and P_0 are the initial spin-down power and period of the pulsar, n the breaking index, I the moment of inertia. The injected particles are confined in the nebula, and the maximum energy of the particles can be expressed by[15]

$$E_{\max}(t) = E_{\max,0}(L(t)/L_0)^{1/2}, \quad (3)$$

where $E_{\max,0}$ is the initial maximum energy, which can be estimated by comparing the model results with the Fermi LAT observation.

The number of the particle contained in the PWN at energy E_e can be expressed as[15]

$$\frac{dN(E_e, T_{\rm age})}{dE_e} = \int_0^{T_{\rm age}} Q(E_e, t)\exp\left(-\frac{T_{\rm age}-t}{\tau_{\rm eff}}\right)dt, \quad (4)$$

where $T_{\rm age}$ is the age of PWN, and $\tau_{\rm eff}^{-1} = \tau_{\rm syn}^{-1} + \tau_{\rm esc}^{-1}$, $\tau_{\rm syn} \approx 1.25\times10^4[B(t)/10\,\mu{\rm G}]^{-2}(E_e/10\,{\rm TeV})^{-1}\,{\rm yr}$ is the lifetime of the relativistic electron of the synchrotron emission loss, $\tau_{\rm esc}(t) \approx 3.4\times10^4[B(t)/10\,\mu{\rm G}](E_e/10\,{\rm TeV})^{-1}(R_{\rm PWN}/1\,{\rm pc})^2\,{\rm yr}$ is escape timescale. $B(t) = B_0/(1+(t/\tau_B)^\alpha)$ is the time-dependent magnetic field in the PWN. In this study, we use $\tau_B = 500\,{\rm yr}$, and $\alpha = 0.5$ similarly to in Zhang *et al.*[15]

The radiative processes include synchrotron radiation and inverse Compton scattering off the ambient soft photons. The emissivity of the synchrotron radiation can be calculated with

$$Q_{\rm syn}(E_\gamma, t) = \frac{2\sqrt{3}e^3 B}{\hbar E_\gamma m_e c^3}\int_0^{\pi/2} d\theta \sin^2\theta \times \int_{E_{e,\min}}^{E_{e,\max}} dE_e J_e(E_e, t) F\left(\frac{E_\gamma}{E_c}\right), \quad (5)$$

where B is the local magnetic field strength, θ is the electron pitch angle, $J_e(E) = J_e(E, T_{\rm age}) = (c\beta/4\pi)dN(E, T_{\rm age})/dE$, $E_c = 4.2\times10^6 hB\gamma_e^2\sin\theta$. $F(y) = y\int_y^\infty dz K_{5/3}(z)$, $y = E_\gamma/E_c$, where $K_{5/3}$ is the modified Bessel function of order 5/3. We use the full Klein–Nishina cross section for relativistic electrons to calculate the emissivity of the inverse Compton process, that is,

$$Q_{{\rm Comp},j}(E_\gamma, t) = 4\pi\int_0^\infty d\epsilon n_j(\epsilon, r)\int_{E_{e,\rm thresh}}^{E_{e,\max}} dE_e \times J_e(E_e, t)F(\epsilon, E_\gamma, E_e), \quad (6)$$

where ϵ is the target photon energy, n_j is the number density of soft photon component j, $E_{e,\rm thresh} = (E_\gamma + [E_\gamma^2 + E_\gamma(m_e c^2)^2/\epsilon]^{1/2})/2$ is the lowest energy that electrons can scatter a target photon with energy ϵ to energy E_γ. The energy distributions of the CMB, IR, and starlight components are given by

$$n_j(\epsilon) = \frac{15U_j}{(\pi kT_j)^4}\frac{\epsilon^2}{\exp(\epsilon/kT_j)-1}. \quad (7)$$

Moreover, the synchrotron radiation of the nebula is supposed to be homogenous with average emission volume $V_0 = 4\pi r_0^3/3$, and the density is $n_{\rm syn}(r,\epsilon) = Q_{\rm syn}(\epsilon)U(x)/4\pi r_0^2 c$, where $U(x) = 3/2\int_0^1 y/x\times\ln[(x+y)/|x-y|]dy$, where $x \equiv r/r_0$. In Ref. [15], r_0 is a free parameter. However, we let it equal to the radius of the nebula, so the number of the parameters is reduced by one in this study. $F(\epsilon, E_\gamma, E_e)$ is expressed as

$$F(\epsilon, E_\gamma, E_e) = \frac{3\sigma_{\rm T}}{4(E_e/mc^2)^2}\frac{1}{\epsilon}\left[2q\ln q + (1+2q)(1-q) + \frac{(\Gamma q)^2(1-q)}{2(1+\Gamma q)}\right], \quad (8)$$

where $\Gamma = 4\epsilon E_e/m^2c^4$, $q = E_1/\Gamma(1-E_1)$, $E_1 = E_\gamma/E_e$ and $1/[4(E_e/mc^2)] < q < 1$.

Crab nebula has an age of 950 yr and a distance of 2 kpc.[19,20] It has been detailedly detected from radio to VHE γ-rays, and, especially, Abdo et al. reported the spectrum obtained by the Fermi LAT in the GeV band. The falling edge of the synchrotron radiation and the rising edge of the inverse Compton scattering of the nebula are clearly revealed by the Fermi LAT,[16] which can better constrain the parameters involved in the model. In the radio and optical observations, the nebula has an angular size of $5\times7\,{\rm arcmin}^2$, which corresponds to a spatial size of $3\times4\,{\rm pc}^2$ for a distance of $d = 2\,{\rm kpc}$. The Crab pulsar PSR B0531+21 centered in the Crab nebula has a spin period of 33 ms, a period derivative $4.23\times10^{-13}\,{\rm s\,s^{-1}}$ with a braking index of 2.51 ± 0.01. The spin-down luminosity of the pulsar is $4.6\times10^{38}\,{\rm erg\,s^{-1}}$, and the character age is $\tau = -P/2\dot{P} = 1230\,{\rm yr}$.[21,22]

When calculating the multiwavelength photon spectrum of the Crab nebula, we take most of the model parameters as the best fitted ones given by Zhang *et al.*[15] We take the initial period of the Crab pulsar as $P_0 = 19\,{\rm ms}$, the braking index $n = 2.5$, the age is 1000 yr.[15] The initial spin-down luminosity is estimated as $L_0 \approx 2.0\times10^{39}\,{\rm erg\,s^{-1}}$ by Eq. (2), here the spin-down power is $L(t) = 4.6\times10^{38}\,{\rm erg\,s^{-1}}$[16] and $I = 10^{45}\,{\rm g\,cm^2}$. The resulting multiband spectrum is sensitive to α_1, α_2 and E_b, so we set $\alpha_1 = 1.5$, $\alpha_2 = 2.5$, $E_b = 150\,{\rm GeV}$ for the Crab nebula, which are consistent with those used by Atoyan and Aharonian.[23] In order to explain the combined results of Fermi LAT and Cherenkov observations above 100 GeV, Abdo *et al.*[16] showed that the magnetic field lies between 100 μG and 200 μG, so we use $B = 150\,\mu{\rm G}$ in our calculation, which also consistent with the estimation by Horn and Aharonian,[18] where $B \sim 140\,\mu{\rm G}$. The soft photons which was scattered by the inverse Compton process include the synchrotron photons

which is the main soft photons with energy above 1 GeV, the 2.7 K CMB radiation with energy density of 0.25 eV·cm^{-3}, the 46 K FIR radiation with energy density of 0.5 eV·cm^{-3}, and the 5000 K starlight with energy density of 1.0 eV·cm^{-3} which consistent with Refs. [15,23]. We compare the modeled spectrum with the observations and obtain the best fitted parameters, which are listed in Table 1 and the resulting multi-band nonthermal emission is given in Fig. 1 with the observed flux points in radio,[7] millimeter and IR,[24–26] optical[8] soft x-rays to γ-rays,[9] VHE γ-rays,[27–29] the γ-rays with energies from 100 MeV to 300 GeV obtained with the Fermi LAT.[16] The nonthermal emission below 100 MeV is from synchrotron radiation of the injected electrons/positrons, whereas the higher energy photons are produced via inverse Compton scattering of these electrons/positrons off the ambient soft photons.

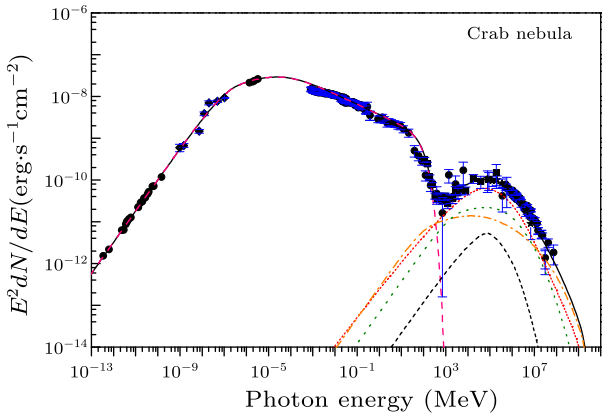


Fig. 1. The resulting total emission (solid line), synchrotron emission (dashed line), and inverse Compton scattering off the synchrotron photons (short-dotted line), the CMB (dash-dotted line), and IR (dotted line), and starlight (short-dashed line). The observed flux points in radio,[7] millimeter and IR,[24–26] optical,[8] x-rays and γ-rays,[9] and VHE γ-rays detected by HEGRA, H.E.S.S.,[27,28] and MAGIC,[29] the 100 Mev to 300 GeV γ-ray data from Fermi LAT[16] are also shown in the figure for comparison.

The initial maximum energy affects the falling edges of the spectrum energy distribution, and the resulting nonthermal spectra for $E_{\rm max,0} = 1.0\times10^3$ TeV, $E_{\rm max,0} = 3.0\times10^3$ TeV, $E_{\rm max,0} = 5.4\times10^3$ TeV, $E_{\rm max,0} = 7.0\times10^3$ TeV and $E_{\rm max,0} = 9.0\times10^3$ TeV with the different fluxes obtained with the Fermi LAT in the GeV band are shown in Fig. 2. The initial maximum of the injected electrons/positrons is constrained to be $\sim 5.4\times10^3$ TeV by comparison of the resulting spectrum with the Fermi result. As shown in Fig. 2, the resulting flux is consistent with the observation presented by Fermi LAT, whereas the result given by Zhang *et al.*[15] overestimated the GeV flux, because a relatively smaller $R_{\rm PWN}$ is used in their calculation.

MSH 15–52 is a shell-like SNR in the radio band, and its northwest region has bright spots coincident with the IR and optical nebula RSW 89.[30,31] Einstein x-ray observations find an elongated nonthermal source centered on the pulsar PSR B1509−58 in MSH 15–52, lately it was confirmed by ROSAT and interpreted as a pulsar wind nebula powered by the pulsar.[10,31] BeppoSAX measured the hard x-ray spectrum of the PWN and the detection of PDS instrument gave a photon index of 2.1 ± 0.2 and a flux of 1.2×10^{-10} erg cm^{-2}s^{-1} in the energy range 20–200 keV for a power-law fit to the unpulsed high-energy flux.[11] The extended VHE γ-ray emission from the asymmetric pulsar wind nebula in MSH 15–52 was discovered by H.E.S.S., and the total energy spectrum from 280 GeV up to 40 TeV can be fitted by a power law with a photon index of $2.27\pm0.03_{\rm stat}\pm0.20_{\rm syst}$.[13] The VHE γ-ray emission has also been detected by CANGAROO-Ⅲ.[14]

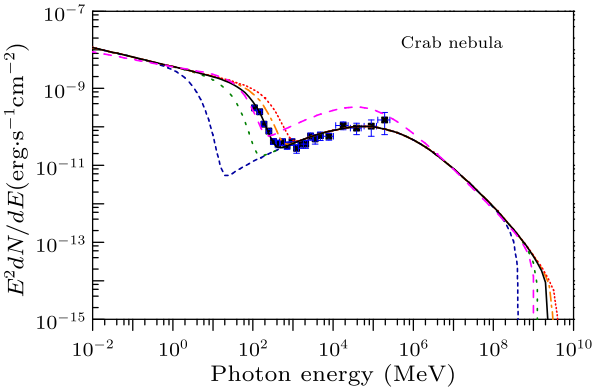


Fig. 2. The resulting spectral energy distribution of the Crab nebula with different initial maximum energy $E_{\rm max,0}$, $E_{\rm max,0} = 1.0\times10^3$ TeV (short-dashed line), $E_{\rm max,0} = 3.0\times10^3$ TeV (dotted line), $E_{\rm max,0} = 5.4\times10^3$ TeV (solid line), $E_{\rm max,0} = 7.0\times10^3$ TeV (dash-dotted line), and $E_{\rm max,0} = 9.0\times10^3$ TeV (short-dotted line). The total emission given by Zhang *et al.*[15] is represented as the dashed line. The flux points obtained with the Fermi LAT[16] from 100 MeV to 300 GeV are also presented.

The pulsar PSR B1509-58, one of the youngest and most energetic pulsars known in the Galaxy, has a rotation period of 150 ms discovered by the Einstein satellite, a large period derivative 1.5×10^{-12} s s^{-1}, a characteristic age of 1700 years, and a spin-down power $\dot{E} = 5.4\times10^{37}$ erg·s^{-1} with a braking index 2.84.[15,31,32] In calculating the photon spectrum of the PWN, we assumed the initial period to be $P_0 = 30$ ms and the spin-down luminosity to be $L_0 = 2.15\times10^{39}$ erg·s^{-1} which is estimated by $L(t) = 5.4\times10^{37}$ erg·s^{-1} with $I = 10^{45}$ g·cm^2 for the pulsar, and the average magnetic field of the nebula is $\sim$ 17 μG estimated by Aharonian *et al.*,[13] and $\alpha_1 = 1.0$, $\alpha_2 = 2.6$, $E_b = 110$ GeV for the broken power-law to consistent with the flux points. The soft photons scattered in the inverse Compton process include the synchrotron photons, the CMB photons, the 35 K IR radiation, and the 5000 K starlight, and all of these are consistent with Abdo *et al.*[17] The details of the best fitted parameters are listed in Table 1, and the resulting multi-band nonthermal emission is given in Fig. 3 with the observed flux points in radio,[12] x-rays,[11] GeV γ-ray,[17] VHE γ-ray.[13,14] The observed

emission in the radio and x-ray bands detected with BeppoSAX can be well explained as the synchrotron radiation of the high-energy electrons/positrons injected in the nebula. Moreover, the resulting inverse Compton scattering off the IR photons is consistent with the γ-rays detected with the Fermi LAT, HESS and CANGAROO-Ⅲ. Notice that the energy distribution spectrum given by Zhang *et al.*[15] is lower than the Fermi data, while our results have a better consistency.

Fermi LAT has detected the gamma-ray emission from the Crab pulsar and PSR B1509-58 and their PWNe, which can provide more information to study the physical properties about the PWNe. Based on the time-dependent injection model of nonthermal emission from PWNe developed by Zhang *et al.*,[15] we study the multiband nonthermal emission from Crab nebula and the PWN in MSH 15–52 with the appropriate parameters shown in Table 1. The GeV emissions given by Fermi LAT can help us to estimate the maximum energy of the relativistic electrons. In our study, we find that it is reasonable to use the radius of the Crab nebula ($R_{\rm PWN} = 2.0$ pc) as the radius of the synchrotron emission, which are different from Zhang *et al.*[15] The reasonable magnetic field of the Crab nebula is $B \sim 150\,\mu$G, which is about half of that in Ref. [15]. The modeled spectrum is more consistent with the observed one given by the Fermi LAT.

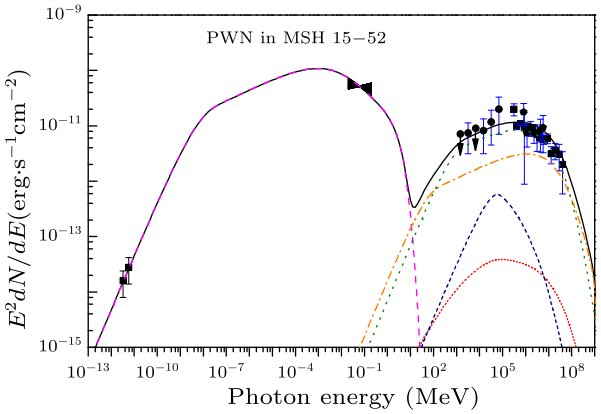


Fig. 3. The resulting total emission (solid line), synchrotron emission (dashed line), and inverse Compton scattering off the synchrotron photons (short-dotted line), the CMB (dash-dotted line), and IR (dotted line), and starlight (short-dashed line). The observed flux points in radio,[12] x-rays,[11] GeV γ-ray,[17] VHE γ-ray[13,14] are shown in the figure for comparison.

Table 1. Values of parameters used in the model.

Model parameter	Symbol	Crab nebula	PWN in MSH 15-52
Distance	d (kpc)	2.0	5.2
Conversion Efficiency	η	0.24	0.2
Initial Spin-Down Power	L_0 (erg s^{-1})	2.0×10^{39}	2.15×10^{39}
Birth Period	P_0 (s)	0.019	0.030
Moment of Inertia	I (g cm^2)	1.0×10^{45}	1.0×10^{45}
Breaking index	n	2.5	2.84
Spectral index 1	α_1	1.5	1.0
Spectral index 2	α_2	2.5	2.6
Present-day B-field	$B(t)$ (μG)	150.0	17.0
Age	$T_{\rm age}$ (yr)	1000.0	1700.0
The initial maximum energy	$E_{\rm max,0}$ (TeV)	5.4×10^3	8.0×10^3
Average PWN radius	$R_{\rm PWN}$ (pc)	2.0	4.0
Break energy	E_b (MeV)	1.5×10^5	1.1×10^5

We would like to thank the anonymous referees, whose comments were very helpful in improving the manuscript. We also thank Professor L. Zhang for his constructive suggestions.

References

[1] Zhang L et al 2007 *Chin. Phys. Lett.* **24** 10
[2] Rees M J et al 1974 *Mon. Not. R. Astron. Soc.* **167** 1
[3] Gaensler B M and Slane P O 2006 *Annu. Rev. Astron. Astrophysics.* **44** 17
[4] Fang J and Zhang L 2010 *Astron. Astrophys.* **515** 20
[5] Fang J and Zhang L 2010 *Astrophys. J.* (in press) (arXiv:1005.3386)
[6] Green D A 2009 *Bull. Astron. Soc. India* **37** 45
[7] Baars J W M et al 1972 *Astron. Astrophys.* **17** 172
[8] Véron-Cetty M P et al 1993 *Astron. Astrophys.* **270** 370
[9] Kuiper L et al 2001 *Astron. Astrophys.* **378** 918
[10] Trussoni E et al 1996 *Astron. Astrophys.* **306** 581
[11] Mineo T et al 2001 *Astron. Astrophys.* **380** 695
[12] Gaensler B M et al 2002 *Astrophys. J.* **569** 878
[13] Aharonian F et al 2005 *Astron. Astrophys.* **435** L17
[14] Nakamori T et al 2008 *Astrophys. J.* **677** 297
[15] Zhang L et al 2008 *Astrophys. J.* **676** 1210
[16] Abdo A A et al 2010 *Astrophys. J.* **708** 1254
[17] Abdo A A 2010 *Astrophys. J.* **714** 927
[18] Horns D and Aharonian F A 2004 *Proceedings of the 5th INTEGRAL Workshop on the INTEGRAL Universe* (ESA SP-552) (Munich, Germany 16–20 February 2004)
[19] Trimble V 1973 *Publ. Astron. Soc. Jpn.* **85** 579
[20] Weiler K W et al 1980 *Astron. Astrophys.* **90** 269
[21] Weekes T C 1992 *Space. Sci. Rev.* **59** 315
[22] Lyne A G et al 1993 *Mon. Not. R. Astron. Soc.* **265** 1003
[23] Atoyan A M et al 1996 *Mon. Not. R. Astron. Soc.* **278** 525
[24] Strom R G and Greidanus H 1992 *Nature* **358** 654
[25] Bandiera R et al 2002 *Astron. Astrophys.* **386** 1044
[26] Green D A et al 2004 *Mon. Not. R. Astron. Soc.* **355** 1315
[27] Aharonian F et al 2004 *Astrophys. J.* **614** 897
[28] Aharonian F et al 2006 *Astron. Astrophys.* **457** 899
[29] Albert J, Aliu E et al 2008 *Astrophys. J.* **674** 1037
[30] Milne D K et al 1993 *Mon. Not. R. Astron. Soc.* **264** 853
[31] Seward F D and Harnden F R Jr 1982 *Astrophys. J.* **256** L45
[32] Livingstone M A et al 2005 *Astrophys. J.* **619** 1046